Electronic structure of metallic superlattices: Mo/V

S. Papadia
Institute of Theoretical Physics, Chalmers University of Technology, S-412 96 Göteborg, Sweden

K. Karlsson and P. O. Nilsson
Department of Physics, Chalmers University of Technology, S-412 96 Göteberg, Sweden

T. Jarlborg
DPMC, Université de Genève, 24 Quai Ernest Ansermet, CH 1211 Genève 4, Switzerland
(Received 19 June 1991)

The electronic structure for a metallic superlattice system, Mo/V, has been calculated using the linear muffin-tin orbital method in the atomic-sphere approximation (ASA). Total energies have been calculated in the local-density approximation (LDA). Emphasis has been given to the electronic-density variation in these materials in order to understand hydrogen storage in metallic superlattices. It is found, within effective-medium theory, that the balance between charge transfer at the interfaces and volume changes of the constituents determines preferred hydrogen sites in Mo/V. Total-energy considerations favor a tetragonal distortion of the Mo/V superlattice over a cubic structure. Results for the LDA bands, charge transfer, and density of states are compared to other electronic-structure calculations of metallic superlattices, which gives rise to a consistent picture of electronic effects in these systems. The dependence of the results on the ASA is discussed.

I. INTRODUCTION

The field of experimental and theoretical studies of artificial structures, in particular multilayered metal films, has expanded rapidly during the last ten years. The magnetic and superconducting properties of such materials were the first effects to be considered since there are striking differences between the layered structures and the constituent metals.[1] There is a significantly enhanced magnetism at the interfaces of certain metallic superlattices (e.g., Fe/V, Cu/Ni, Cr/Au) and the superconducting temperature, T_o, was found to increase for certain artificially layered metal structures. The discovery of high-temperature ceramic superconductors changed the focus in the field of metallic superlattices from trying to fabricate high-temperature metallic multilayered superconductors to trying to understand the role of layering on the superconductivity. Another very peculiar and controversial property of metallic superlattices is the so-called supermodulus effect. It was claimed that the biaxial elastic modulus in certain metallic superlattices is greatly enhanced[2]—up to 400%. There have been many attempts to verify and explain the phenomenon. An excellent review of the activities up to 1986 is given by Terakura in Ref. 1. The controversy still exists, and there is ongoing experimental and theoretical work on the subject.[3–8]

An unexplored area in this field is the chemical properties of multilayered structures (e.g., catalytic properties, chemisorption and absorption of species in such materials). Some studies on hydrogen loading and absorption in metallic superlattices have been made[9–11] where different aspects have been addressed. In Nb/Ta, the hydrogen solubility was found to increase compared to the bare metals.[10] In addition, the effects of a modulated hydrogen composition on the hydrogen-metal phase transitions were explored. It was found that the critical fluctuations of the hydrogen density are suppressed if the fluctuation wavelengths are shorter than the superlattice periodicity, which results in a suppression of the gas-liquid phase transition of hydrogen in the Nb layers. Hydrogen loading in Mo/V systems has recently been studied.[11] Here, the hydrogen composition modulation is expected to be very pronounced since hydrogen dissolves in the vanadium metal but not in the molybdenum metal. The hydrogen solubility in the vanadium layers was found to decrease compared to the bulk vanadium and the question was raised about the electron-density-distribution effects on the hydrogen solubility, especially at the interfaces.

We address this question in the following by calculating the electronic structure of Mo/V. A more general aim is to understand the valence-electron-character and geometric-structure effects on the electron structure in metallic superlattices since this is a first step towards an understanding of the physical properties of such materials. An interesting viewpoint is to unify the knowledge from different systematic studies into a consistent physical picture of what happens in artificially layered structures.

The Mo/V growth seems to be particularly easy to control which makes it possible to fabricate very-well-characterized structures with sharp interfaces, to such an extent that even well-defined quasiperiodic superlattices have been grown and studied.[12,13] The good quality of these superlattices is promising also from a theoretical point of view since we, with some justification, may disregard interdiffusion at the interfaces—the main deviation from perfectly layered structures. We study, in the fol-

lowing, the electron structure of perfect-interface $(Mo)_n(V)_n$ superlattices, with $n=1$, 3, and 5, and focus on the charge-transfer and lattice-structure effects on the electron-density distribution. The hydrogen solubility is coupled to the electron-density distribution according to effective-medium theory (EMT),[14,15] where the binding energy of an impurity is to the largest extent determined by the surrounding electron density. We also compare results for band structure, charge transfer, and density of states with earlier calculations for the Nb/Zr system[16] and find that a consistent picture for basic mechanisms in metallic superlattices arises. The present calculations are made in the linear muffin-tin orbital (LMTO) scheme[17] within the atomic-sphere approximation (ASA). Total energies have been calculated in the local-density approximation of Hedin and Lundqvist.[18]

The rest of the paper is organized as follows. In Sec. II, the technical details of the implementation of the LMTO-ASA scheme on this particular problem are presented. In Sec. III A, the results for the band structure for bulk Mo, bulk V, and $(Mo)_n/(V)_n$ superlattices are presented and discussed. Comparisons are made with other calculations for the bulk material properties (equilibrium volume, band structure, density of states). The results for the total and local density of states for the superlattices are discussed in Sec. III B. In Sec. III C, the coupled quantities—interstitial-density variation and charge transfer in the $(Mo)_n/(V)_n$ superlattices—are discussed. The hydrogen solubility in these materials is then explored within effective-medium theory for hydrogen heat-of-solution in transition metals. Total-energy calculations for different possible geometric structures of the $(Mo)_n/(V)_n$ superlattices are presented in Sec. III D. Calculated total-energy differences are used to distinguish between different crystal structures. A summary and the main conclusions are finally given in Sec. IV.

II. IMPLEMENTATION OF THE CALCULATIONS

In this section, we describe the unit cells of the $(Mo)_n/(V)_n$ superlattices, the calculation of the density of states, the definition of charge transfer, the calculation of the interstitial density variation, and the total-energy calculations.

The basis set used in all calculations is the conventional LMTO basis set with nine orbitals (*spd*) per atom. Relativistic effects, except spin-orbit coupling, are taken into account for the valence electrons. All core electrons are included in the calculations and are treated fully relativistically.

The unit cell for Mo and V in the bulk materials is body-centered cubic (bcc). We sample 572 **k** points in an irreducible part of the first Brilloun zone and choose the atomic sphere radius around each atom to be the Wigner-Seitz radius. The simplest superlattice, indicated by $(Mo)_1/(V)_1$, consists of one monolayer of each of the constituent metals, and is grown in the (100) direction—the z direction in Fig. 1. Its unit cell is the simple cubic (sc) with a basis. We sample 125 **k** points and choose the volumes of the Mo and V spheres in every superlattice unit cell to be equally large and the sum of their volumes

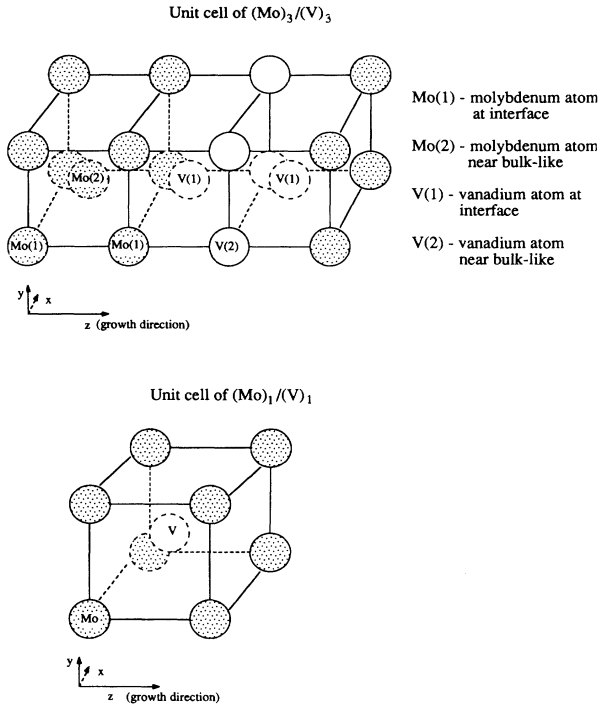

FIG. 1. Unit cells of $(Mo)_3/(V)_3$ and $(Mo)_1/(V)_1$ superlattices. The shaded atoms are Mo atoms, and the unfilled atoms are V atoms. The atoms labeled Mo and V [or Mo(1), Mo(2), V(1), and V(2)] are the ones constituting the unit cells.

to equal the unit cell volume. The unit cells for $(Mo)_3/(V)_3$ (seen in Fig. 1) and $(Mo)_5/(V)_5$ are tetragonal with six and ten atoms, respectively, in the unit cell. For these structures, we sample 75 **k** points.

The bulk structures are represented both as bcc and as sc with a basis. We calculate the band structure for the bcc bulk structures in the Γ-H direction and for the $(Mo)_n/(V)_n$ superlattices in the Γ-Z direction. The Γ-Z direction corresponds to the Γ-H direction but extends only partly along it, e.g., for the $(Mo)_1/(V)_1$ superlattices, the Γ-Z direction extends half the way along the Γ-H direction. The band structure of the bulk sc materials is also calculated in the Γ-Z direction. The density-of-states curves of bulk Mo, bulk V, and $(Mo)_n/(V)_n$ superlattices are calculated using a tetrahedron integration routine.[19]

The charge transfer can be defined in several ways. The definition of charge transfer within the ASA makes this quantity dependent on the radius of the atomic sphere. The *difference* in charge transfer in different systems is though a more relevant quantity, provided that the sphere radii are the same in all the calculations. The (negative) charge transfer from a particular atom is here defined as the charge ionicity of the atom. Denoting the atomic charge of the nucleus in an atomic sphere S as Z_S, and the integrated self-consistent (negative) charge as Q_S, the ionicity is given by $Z_S - Q_S$.

If we follow the requirement that the sphere radii should be chosen so as to minimize the total energy of the

chosen structure,[17] we find, for the $(Mo)_1/(V)_1$ superlattice, that a choice of equal atomic sphere volumes is the best one in the simple cubic unit cell, whereas for a tetragonal cell there are better choices. In "tetragonal" superlattices, contracted in the growth direction, the best sphere radius choice is a somewhat larger molybdenum atomic sphere (of about 0.5% compared to the vanadium atomic sphere radius). On the other hand, for tetragonal $(Mo)_1/(V)_1$ superlattices, expanded in the growth direction, the best choice of sphere radii is a somewhat smaller molybdenum atomic sphere radius compared to the vanadium atomic sphere radius. The different choices of sphere radii quoted above did not affect any final results apart from a negligible difference in the charge transfer quantity. The reasons for that are that the sphere sizes did not differ much, but also that the inclusion of overlap terms has the effect of correcting in the boundary region between spheres. We have in the present calculations always chosen equal sphere radii for the tetragonal $(Mo)_n/(V)_n$ materials in order to keep as many parameters as possible fixed, in favor of controlled total energy comparisons.

We explore the spatial electron-density distribution in order to get a first indication of where hydrogen would most likely dissolve in the $(Mo)_n/(V)_n$ superlattices. We probe the electron density in the region between the muffin-tin radius and the atomic-sphere radius—the interstitial region in the ASA. This region is the relevant one since the hydrogen atom prefers to sit in a symmetric (interstitial) site in a metal lattice. Usually, the density in the interstitial region is, within the ASA, calculated by averaging the contributions of all atoms in the unit cell over the interstitial space. In a cell with many atoms, as in the $(Mo)_3/(V)_3$ and $(Mo)_5/(V)_5$ superlattices, a density variation in the real material is expected also in the interstitial region, depending on between which atoms we choose to probe the density. To estimate the density variation, we calculate the density in the interstitial region around a certain atom in the unit cell by averaging only the tail contributions of nearest-neighbor atoms.

The total energies are calculated as usual in the LMTO-ASA method,[20] but with the Madelung contribution calculated according to Jarlborg and Arbman.[21] The use of an approximate functional due to the restrictions on the potential (in the ASA, the potential is constructed from a spherically averaged trial charge density) gives, evidently, not the correct *total* energy. The energy *differences* are still significant since the functional is exactly minimized. The Hedin-Lundqvist[18] local-density approximation is used for the exchange and correlation part of the effective potential.

We use a quadratic minimization scheme for finding the $(Mo)_1/(V)_1$ sc structure with lowest energy. The minimization parameters are the lattice constant and the sphere radii. All other input parameters are restricted to have the same values in all the calculations to favor controlled total-energy comparisons. The calculated total energies lie very close so we need a convergence of 0.1 mRy in the total-energy values. The numerical accuracy in the total-energy calculations is then ± 1 meV. The efficiency of the quadratic interpolation scheme compensates for the slow convergence; we only need to calculate total energies for four different lattice constants and four different choices of atomic sphere radii to achieve the optimum parameter values for cubic $(Mo)_1/(V)_1$.

The quadratic minimization in the calculations for finding the optimum tetragonal structure of $(Mo)_1/(V)_1$, is employed in a slightly different way. Now the varied parameters are the length of the c- axis (the axis along the growth direction) and the length of the axis parallel to the growth direction. The atomic sphere radii are chosen to be equal. We fit a two-dimensional quadratic function $f(x,z)$ to the energy values corresponding to the different choices of axis lengths. In doing that, we obtain a 6×6 matrix equation for the coefficients of the function which is solved, giving the variables x ad z for which $\nabla f=0$.

III. RESULTS AND DISCUSSION

A. Band structure

We calculate the band structure in the Γ-Z direction of Mo bulk, V bulk, and $(Mo)_n/(V)_n$ superlattices. Mo and V in bulk have bcc structures with experimentally determined lattice constants of 3.15 and 3.02 Å, respectively.[22] We determine the equilibrium lattice constant for bulk Mo and V predicted by the LMTO-ASA calculations by comparing the total pressure in the unit cell. The equilibrium lattice constant is given for vanishing total pressure.

The volume (lattice constant) dependence of the total pressure in the unit cell is shown in Fig. 2. The resulting equilibrium lattice constants are 3.19 Å for Mo and 2.99 Å for V, which differ by 2% and 1%, respectively, compared to the experimentally measured ones.

We compare our calculations for equilibrium lattice constant to independent Korringa-Kohn-Rostoker (KKR) calculations by Morruzzi, Janak, and Williams.[23] The equilibrium lattice constants of Mo and V given by the KKR calculations are 3.12 Å and 2.93 Å, respective-

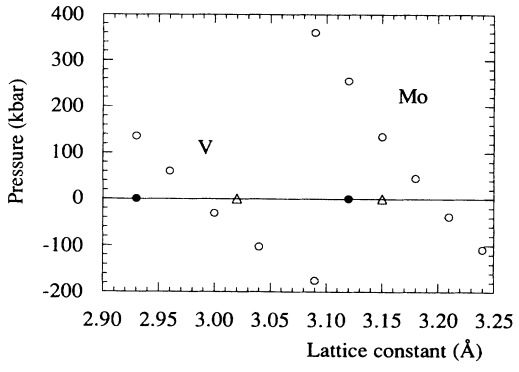

FIG. 2. The total pressure vs lattice constant for molybdenum and vanadium bcc crystals. The equilibrium lattice constants are given for zero pressure. The leftmost values correspond to V and the rightmost values correspond to Mo. The present work is marked with ○; the ● denotes the calculation of Moruzzi, Janak, and Williams in Ref. 22; the △ indicates the experimental values for equilibrium lattice constants.

ly, which differ from the LMTO-ASA calculations by 2%. Since the KKR equations are related to the LMTO equations,[17,24] the main source for the discrepancy is the approximation of overlapping spheres and the linearization of the eigenvalue equations in the LMTO-ASA—absent in the KKR calculations. We expect that the ASA, and not the linearization, is the approximation giving the largest error compared to the KKR method. Overlap corrections ("combined correction" terms) and extended basis make the calculations agree with the KKR results, as can be compared in Barbiellini, Moroni, and Jarlborg.[25] Calculations of equilibrium volumes in the local-density approximation (LDA) which do not use the muffin-tin approximation for the potential report better agreement with experimental values—within 1% for norm-conserving pseudopotentials[26] and 1–4% for full potentials in a linear augmented-Slater-type-orbital method.[27] Note that we compare volumes here instead of lattice constants. It is interesting to note the tendency to underestimate the equilibrium volume,[23,27] by an increasing amount with smaller atomic number and especially for materials on the left-hand side of the Periodic Table (comparing only those materials that have been calculated for the same structure as the experimentally observed ones). On the other hand, there exists a breakpoint for large atomic numbers (around 45)[23] where an overestimation occurs. This is compensated with the account of (scalar-)relativistic effects[27] which tend to "shrink" the core radius.[26] Inclusion of spin-polarization effects via the local-spin-density approximation give the opposite trend—the equilibrium lattice constant increases.[23]

The calculated band structures in the Γ-Z direction and the total density-of-states (DOS) curves for Mo and V with our calculated equilibrium lattice constants are shown in Fig. 3. They compare favorably to the corresponding curves of Moruzzi, Janak, and Williams,[23] which underscores the insensitivity of the band structure to the difference in the calculated equilibrium lattice constants.

The Fermi energy relative to the valence-band bottom (or bandwidth) for Mo and V with different choices of lattice constants is shown in Table I. Note the bandwidth increase for lattice contraction and, correspondingly, the decrease for lattice expansion, an effect seen also in calculations for Nb/Zr superlattices by v. Leuken *et al.*[16] When comparing the calculated density of states for different lattice constants, we find that the main features are similar, but we notice a change in the character of the valence electrons. As the lattice is expanded, slightly more electrons assume free-electron-like (s and p) character. Expansion of the lattice would thus favor some delocalization of the valence electrons, and a contraction would favor a localization—also consistent with the results of v. Leuken *et al.*[16]

The $(Mo)_n/(V)_n$ superlattices are grown coherently,[12,28] which means that, up to a certain thickness, the Mo layers and the V layers adjust to each other in the layer plane (xy plane in Fig. 1), and there exists a mean lattice constant, common to both materials in that plane. Studies for coherently grown semiconductor superlattices

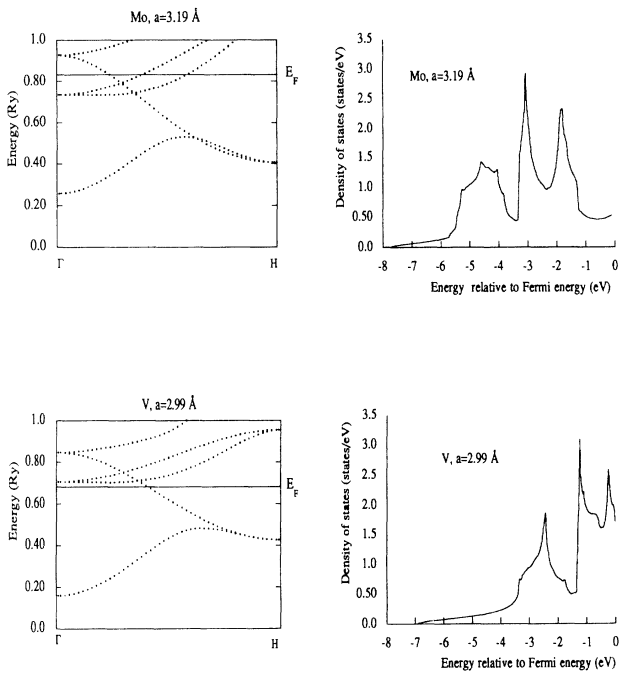

FIG. 3. The band structures in the Γ-H direction, and the total density of states of Mo and V with the calculated equilibrium lattice constants of 3.19 and 2.99 Å, respectively.

and simulations for superlattice growth[29,30] indicate that the lattice constant in a coherently grown superlattice is, within 1%, the arithmetic mean of the equilibrium constants of the constituent materials. In our case, it gives a lattice constant for $(Mo)_n/(V)_n$ of 3.09 Å. To begin with, we choose the axis in the growth direction to be equal to the axes parallel to it, assuming a cubic structure. The effects of a possible tetragonal distortion will be treated in connection with total-energy considerations.

TABLE I. Value of Fermi energy relative to the valence-band bottom vs lattice constant in bulk molybdenum, bulk vanadium, and $(Mo)_n/(V)_n$ superlattices.

Material	Lattice constant (Å)	Fermi energy (Ry)
Mo	3.09	0.60
	3.12	0.59
	3.19	0.57
V	2.93	0.52
	2.99	0.51
	3.02	0.50
	3.09	0.49
$(Mo)_1/(V)_1$	3.09	0.52
$(Mo)_3/(V)_3$	3.09	0.55
$(Mo)_5/(V)_5$	3.09	0.56

The results for the band structures in the Γ-Z direction of bulk Mo, bulk V, and the $(Mo)_1/(V)_1$ superlattice—all with a lattice constant of 3.09 Å— are shown in Fig. 4. The bulk structures of Mo and V are here represented as sc with one extra atom in the middle of the cell. This introduces an extra Bragg plane in the reciprocal cell, compared to the bcc structure, where the bands are folded back (compare with Fig. 3; note the difference in lattice constants which makes a difference in the energy position of the bands). In the band structure for $(Mo)_1/(V)_1$, we distinguish a band with a clear s character that starts at 0.2 Ry (see Fig. 4), a distinct d character band around the Fermi level, and a hybridized band. Note the energy splitting of 0.08 Ry (1 eV) of the s band at the Brillouin-zone boundary due to the potential difference of Mo and V, characteristic for layered structures of different materials.[16,31] In the band structures for the $(Mo)_3/(V)_3$ and $(Mo)_5/(V)_5$ superlattices with lattice constant of 3.09 Å, even more Bragg planes are introduced in the reciprocal cell—two extra planes for $(Mo)_3/(V)_3$ and four extra planes for $(Mo)_5/(V)_5$ in the Γ-Z direction. The multiple band folding in the zone makes it difficult to follow particular bands. The energy splitting of the bands at the extra Bragg planes is still noticed.

The Fermi energy (or bandwidth, according to our definition above) for $(Mo)_1/(V)_1$ with the overall lattice constant of 3.09 Å is 0.52 Ry compared with 0.60 Ry for Mo and 0.49 Ry for V with the same lattice constant (see Table I). If the DOS shapes for the constituent atoms do not change much, then the superlattice-bandwidth con-

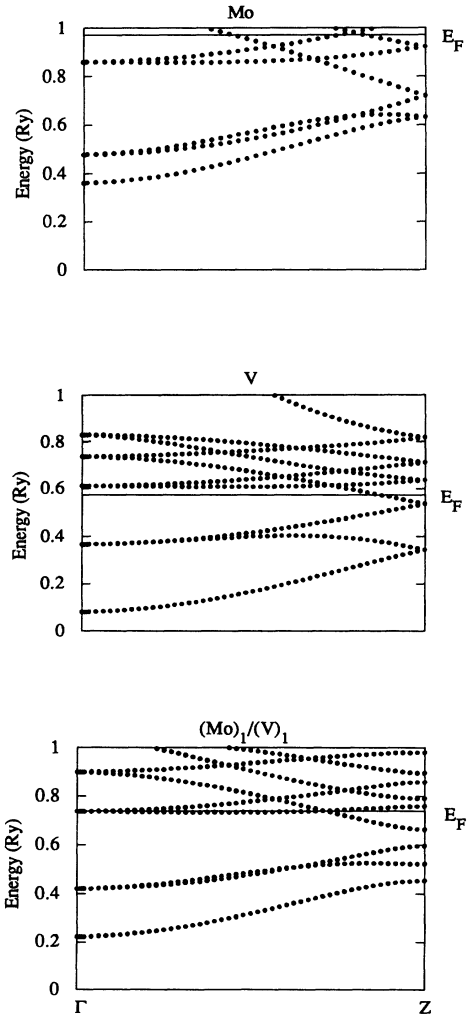

FIG. 4. The band structures in the Γ-Z direction of bulk Mo, bulk V, and $(Mo)_1/(V)_1$ superlattice, all having a lattice constant of 3.09 Å. The structures of bulk Mo and V are here represented as sc with a basis.

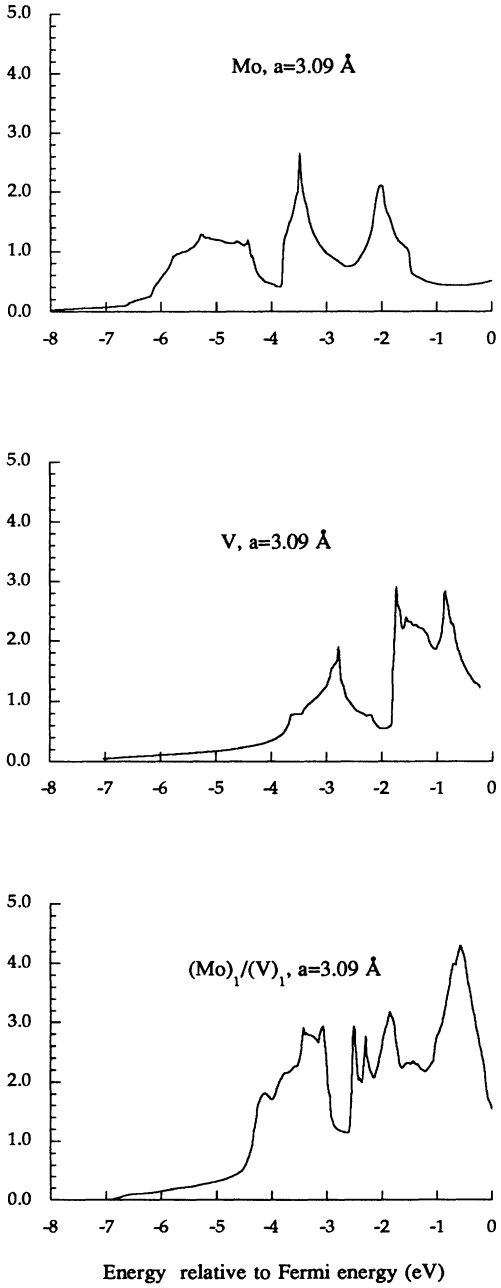

FIG. 5. The total density-of-states curves for bulk Mo, bulk V, and the $(Mo)_1/(V)_1$ superlattice, all with a lattice constant of 3.09 Å.

traction relative to bulk Mo (and expansion relative to bulk V) is an indication of electron transfer from Mo to V in the superlattice. The Fermi energy (bandwidth) for $(Mo)_3/(V)_3$ is 0.55 Ry and for $(Mo)_5/(V)_5$ it is 0.56 Ry. Seemingly,the bandwidth increases with larger superlattice unit cell. This may be coupled to the amount of electron transfer between Mo and V atoms. The larger the Fermi energy of $(Mo)_n/(V)_n$, the lesser the electron transfer at the molybdenum-vanadium interface.

B. Density of states

The total-density-of-states (DOS) curve for $(Mo)_1/(V)_1$ is shown in Fig. 5 together with the total-DOS curves for bulk Mo and V with the same lattice constant as $(Mo)_1/(V)_1$ (3.09 Å). It seems that the DOS for $(Mo)_1/(V)_1$ is approximately a superposition of the DOS of the constituents. In order to make a more detailed comparison, we show in Fig. 6 the local-density-of-states (LDOS) curves for bulk Mo and V with calculated equilibrium lattice constants *and* with a lattice constant of 3.09 Å. The LDOS for Mo and V in $(Mo)_1/(V)_1$ (3.09 Å) is also shown. The effects on the LDOS for the bulk materials due to the volume change manifest mainly in changes of the valence-band widths— a narrowing of the *d* and *p* bands for vanadium and a corresponding widening for the molybdenum bands—when changing the lattice constants from equilibrium bulk values to 3.09 Å. The molybdenum bands seem also to undergo a shift to lower energies. For the LDOS of $(Mo)_1/(V)_1$, we notice a shift to lower energies for V, relative to its bulk LDOS, and for Mo a corresponding shift to higher energies. The intensities of the molybdenum *s* and, especially, *p* electrons have diminished in the superlattice, compared to

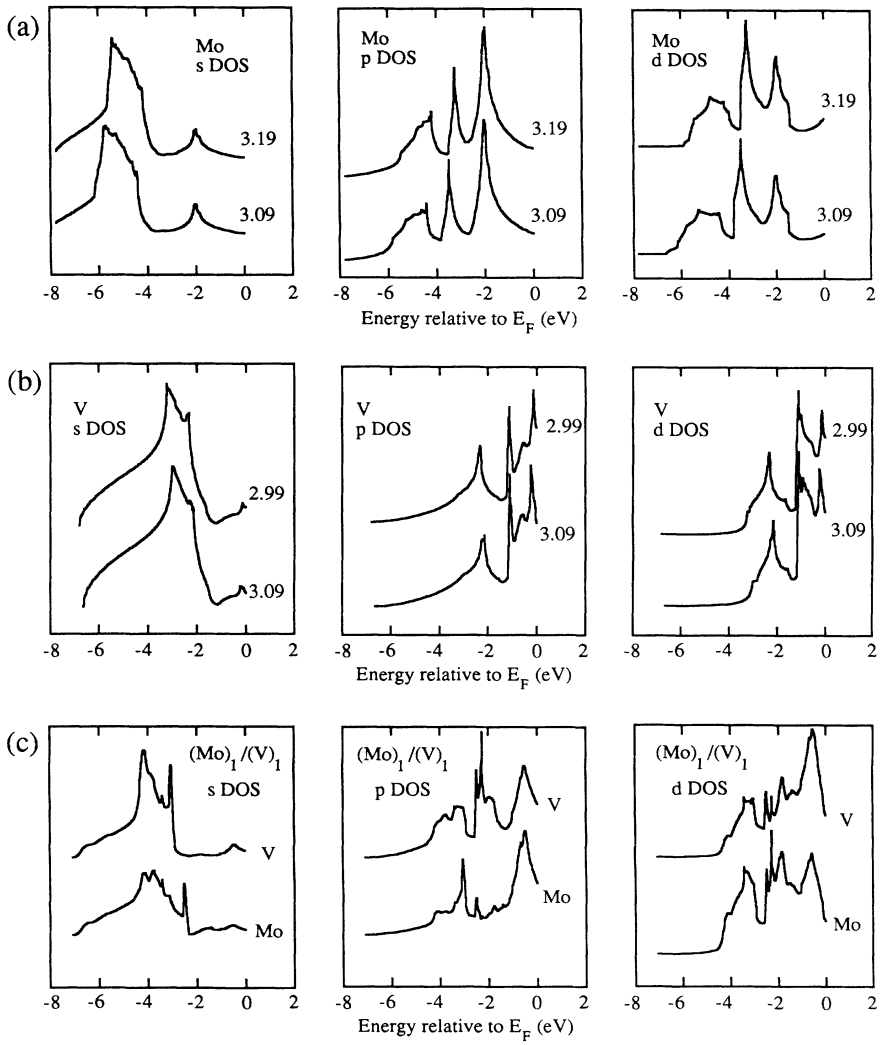

FIG. 6. In (a) is shown the local-density-of-states curves for bulk Mo with calculated equilibrium lattice constant (3.19 Å) and a lattice constant of 3.09 Å. The local-density-of-states curves for bulk V with calculated equilibrium lattice constant (2.99 Å) and a lattice constant of 3.09 Å is shown in (b), and in (c) is shown the local-density-of-states curves for Mo and V in the $(Mo)_1/(V)_1$ superlattice with a lattice constant of 3.09 Å.

the bulk material. Correspondingly, the *s* and *p* intensities of vanadium in the superlattice have increased which is an illustration of *sp*-electron transfer from Mo to V in the Mo/V superlattices.

The LDOS for interface, near interface and bulklike Mo and V in superlattices with larger periodicity are shown in Fig. 7. For the valence *s* electrons, we notice a shift in the *s*-electron "center of gravity" when comparing interface atoms and bulklike atoms. The shift is downwards in energy for interface vanadium and upwards in energy for interface molybdenum with respect to the bulklike atoms. The positions of the *s*-electron peaks for bulklike atoms in the superlattices coincide almost with the corresponding positions of the bulk materials, but their shapes have not adopted the "bulk shape" even for the bulklike positions of Mo and V atoms in the superlattices with largest periodicity.

For the valence *p* electrons of vanadium, there seems to occur a redistribution over the energy range when going from bulklike to interface atoms so as to broaden the *p* band of bulklike vanadium. That indicates stronger *sp* hybridization and less *pd* hybridization for the interface vanadium atoms compared to the bulklike ones. The *p* electrons in molybdenum distribute to energies closer to the Fermi level, when going from bulklike to interface layers, and the *p*-electron intensity diminishes—*p*-electron transfer occurs from Mo to V at the interface.

The valence *d* electrons in the superlattices redistribute to higher energies for Mo and lower energies for V when going from bulklike to interface layers, but the peaks are rather rigid in shape, in contrast with the *sp* peaks. Compared to the bulk materials, the most striking difference of the *d* bands in the superlattices is the narrowing (vanadium) and broadening (molybdenum) of the bandwidth. This is understood as an effect of the local volume changes; for V, the volume has increased relative to its bulk value which results in the narrowing of the *d*-electron-band width, and the opposite is true for Mo. This fact manifests in the separation of *d*-electron peaks of Mo, most clearly seen at the lower energy range, and in the contraction of the vanadium *d*-electron peaks in the superlattices.

The redistribution in energy of the valence electrons when going from bulklike to interface atoms in the superlattices may be seen as an adjustment procedure, referred to as "matching" by v. Leuken *et al.*[16]

C. Interstitial density variation and hydrogen solubility

We clearly see an electron transfer from molybdenum to vanadium at the superlattice interface, some excess electrons on the bulklike Mo atoms, and some lack of electrons on the bulklike V atoms. The results are sum-

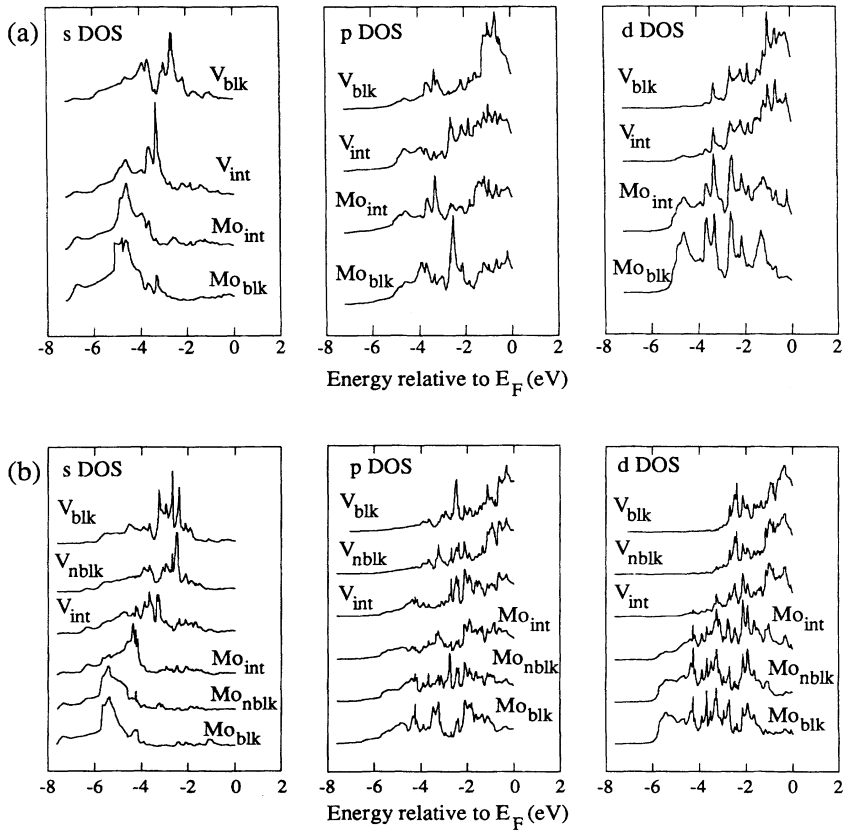

FIG. 7. The local-density-of-states curves for Mo and V in $(Mo)_3/(V)_3$ is shown in (a), and in (b) is shown the corresponding curves for $(Mo)_5/(V)_5$. The lattice constant is 3.09 Å. The subscripts int, blk, and nblk denote interface, bulklike, and near bulklike positions, respectively, of the atoms.

marized in Table II. The charge oscillation seen here, also seen in Nb/Zr by v. Leuken *et al.*,[16] is a typical response of an electron gas to a formation of a dipole layer due to an abrupt change in the potential, which we have at the superlattice interface. We expect the oscillations to assume the typical Friedel oscillation wavelength at larger distances from the interface in electron structure calculations for superlattices with larger periodicity.

The amount of charge transfer at the interface seems to decrease with larger superlattice periodicity and to saturate. That leads also to a saturation of the Fermi energy, which we coupled to the amount of charge transfer in Sec. III A. For $(Mo)_1/(V)_1$ with lattice constant equal to 3.09 Å, the electron depletion for molybdenum at the interface is 0.34 electrons whereas the respective electron loss in $(Mo)_3/(V)_3$ and $(Mo)_5/(V)_5$ is 0.11 electrons.

The results for the interstitial density variation in the larger $(Mo)_n/(V)_n$ supercells are shown in Fig. 8. We have an overshoot and undershoot of the density around the values for the interstitial electron density in bulk Mo (0.040 electrons/a.u.^{3}) and bulk V (0.032 electrons/a.u.^{3}), both with a lattice constant of 3.09 Å. This is a reflection of the charge-transfer situation in the superlattices.

The interstitial densities for bulk molybdenum and vanadium, with calculated equilibrium lattice constants, are 0.037 and 0.035 electrons/a.u.^{3}, respectively. The absorption energies for hydrogen in these metals are -0.26 eV/H for vanadium[32] and 0.45 eV/H for molybdenum,[33] which means that hydrogen dissolves in vanadium but not in molybdenum. In an effective-medium (EMT) approach for explaining the difference in hydrogen heats of solution, Nordlander, Nørskov, and Besenbacher[15] consider the effect of the surrounding electron density—the key parameter in the model—on the hydrogen atom in a transition metal. In the work of Nordlander, Nørskov, and Besenbacher,[15] the hydrogen impurity is embedded in a homogeneous electron gas (jellium) and the absorption energy is calculated, within the LDA, as the difference between the total energy of the hydrogen-in-jellium system and the sum of the total energies of the electron gas and the free hydrogen atom. Then the contributions to the absorption energy due to the differences between the model problem and the real situation (hydrogen in a transition metal) are treated perturbatively. These contributions come in as core corrections, hybridization effects, and lattice relaxation effects. In practice, this scheme works best for close-packed situations (see Zwartkruis and Himbergen[34] for a critical discussion). In our case where we compare hydrogen absorption in two similar metals of the same structure, we have confidence in the qualitative results of Nordlander, Nørskov, and Besenbacher.[15] The absorption energy of hydrogen-in-metal, E_{abs}, is related to the hydrogen heat-of-solution, E_{HOS}, and the H_2 binding energy, E_{H_2}. It is given by $E_{abs}=E_{HOS}+\frac{1}{2}E_{H_2}$. For hydrogen in Mo and V the difference in the value of their interstitial density is the main cause for the different hydrogen heats of solution in these materials since the total total-energy correction for the other effects (hybridization, core repulsion, lattice relaxation) only adds up to 0.04 eV for vanadium and 0.07 eV for molybdenum. For both metals, these corrections lower the hydrogen heat of solution. Following the results of Nordlander, Nørskov, and Besenbacher,[15] the

TABLE II. Electron transfer in $(Mo)_n/(V)_n$ superlattices. The electron transfer is defined in Sec. II B and the different types of atoms are depicted in Fig. 1. The amount of valence electrons in the atomic sphere is shown to illustrate the coupling to the interstitial density variation shown in Fig. 8.

Superlattice (notation)	Type of atom (position)	Electron transfer (electrons/atom)	Valence electrons
$(Mo)_1/(V)_1$	Mo at interface	−0.34	5.66
	V at interface	0.34	5.34
$(Mo)_3/(V)_3$	Mo at interface	−0.11	5.89
	Mo near bulk	0.10	6.10
	V at interface	0.12	5.12
	V near bulk	−0.11	4.89
$(Mo)_5/(V)_5$	Mo at interface	−0.11	5.89
	Mo near bulk	0.14	6.14
	Mo bulk	0.10	6.12
	V at interface	0.13	5.13
	V near bulk	−0.14	4.86
	V bulk	−0.12	4.88

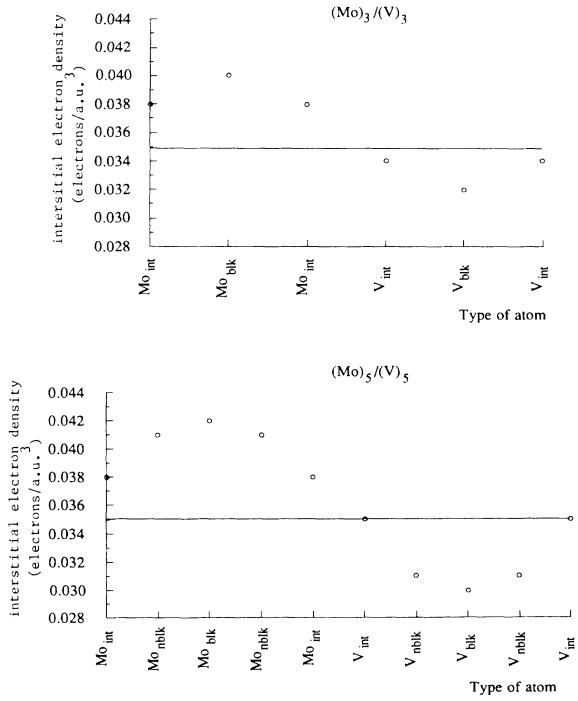

FIG. 8. The values of the interstitial electron density for different types of atoms in the $(Mo)_3/(V)_3$ and $(Mo)_5/(V)_5$ superlattices with a lattice constant of 3.09 Å are shown. The notations int, blk, and nblk denote interface, and bulklike, and near bulklike positions, respectively, of the atoms. The full horizontal line at the value of 0.035 electrons/a.u.^{3} indicates that hydrogen dissolves at and below that limit.

conclusion is that for sites with electron density lower than 0.035 electrons/a.u.^{3} (V equilibrium bulk interstitial density), hydrogen will dissolve, and for sites with density higher than 0.037 electrons/a.u.^{3} (Mo equilibrium bulk interstitial density), hydrogen solution is not preferred. The implications for the $(Mo)_n/(V)_n$ superlattices are then that hydrogen will dissolve in interstitial (tetrahedral) sites in a vanadium layer, even in the interface vanadium layers. To clarify: at tetrahedral sites with an environment of three vanadium atoms and one molybdenum atom, i.e., half a lattice constant away from the interface molybdenum layers, hydrogen solution is preferred. The hydrogen concentration in the vanadium layers is expected to be modulated since the absorption energy is most negative in the bulklike vanadium layers. The present discussion is valid in the presence of perfect interfaces, small lattice distortions, and small hydrogen-hydrogen interaction effects, i.e., small concentration of hydrogen corresponding to the α phase.

The discussion in Hjörvarsson *et al.*[11] concerns the interface effects in Mo/V superlattices on hydrogen uptake. The hydrogen concentration in the vanadium layers in Mo/V is found to diminish drastically close to the interfaces. It is extracted that there is a hydrogen-free layer of 2–3 lattice spacings at the Mo/V interface. By arguments of EMT, this is believed to be due to electron-density increase because of electron transfer from Mo. At first it seems reasonable to assume that the electron-density is increased—and hydrogen solubility diminished—in the interface vanadium layers due to electron transfer from molybdenum. There is, though, a compensating effect—the expansion of the volume that vanadium undergoes when forming a coherent superlattice with molybdenum—resulting in an interstitial-electron-density decrease. The amount of electron transfer is not the same for all kinds of superlattices, as we already have seen (depicted in Table II). The smaller the superlattice periodicity, the larger the electron transfer at the interfaces, which means that there is a higher interface electron density for small-periodicity superlattices. In particular, the interface vanadium interstitial density in $(Mo)_3/(V)_3$ is 0.034 electrons/a.u.^{3}, whereas for $(Mo)_1/(V)_1$ it is 0.036 electrons/a.u.^{3}. The conclusion in the present work, where a self-consistent interstitial density is extracted, is that it is possible for hydrogen to dissolve close to the interface in superlattices of a periodicity of at least three layers of each constituent. If it fails to do so, the reason is not increased electron density at the interfaces but should be sought in deviations from perfect interfaces and possible changes in the H-H interactions for larger hydrogen concentrations. The hydrogen heat of solution in the bulklike vanadium layers in the Mo/V superlattices should not be destructively affected by the layering, but rather increase due to the expansion of the vanadium volume.

D. Total-energy calculations

As discussed earlier, the LMTO method in the atomic-sphere approximation (ASA) has a limited accuracy in the computed *total* energy but energy *differences* are more reliable as long as we consider close-packed, highly symmetric structures.[35] For more open structures, the results become uncertain. It has been found by Skriver[36] that, for V and Mo, the reproduction of the equilibrium bcc structures is possible within the ASA. In addition, calculated total-energy differences between fcc and bcc structures by Barbiellini, Moroni, and Jarlborg[25] agree well with what is generally obtained with similar methods. We consider here superlattices of Mo and V which have the additional complication of possessing an interface where the use of spherical potentials may be questioned. We argue that if no geometrical relaxation is considered across the interface between Mo and V layers, the $l=1$ terms in the potential are reasonably small. That Mo and V have unequal potentials is not as crucial as geometric relaxation since the difference in potential (and charge) is more important in the interior of the muffin-tin (MT) spheres. The sensitivity to geometrical changes is a reason to keep the MT spheres at the Mo/V interfaces of equal size. With the above in mind, we limit the present total-energy considerations of the Mo/V superlattices to perfect-interface bcc structures and tetragonal structures that do not depart much from cubic cells.

We consider the simplest "superlattice"—the $(Mo)_1/(V)_1$—having sc and tetragonal unit cell with a basis. For the sc superlattice, total-energy calculations give minimum total energy for a lattice constant of 3.07 Å and a choice of equal volumes of the atomic spheres in the unit cell. The values for the total energy of sc $(Mo)_1/(V)_1$ for different lattice constants are shown in Table III. The energy values are given as the difference between the sum of the total energies of bulk Mo and V with calculated equilibrium constants and the total energy of the superlattice unit cell (containing one Mo and one V atom). It should be kept in mind that the numerical accuracy is ± 1 meV when comparing the calculated energy values. The total pressure is also tabulated and its variation with lattice constant is consistent with the total-energy values. We notice immediately that the superlattice structures are stable (or metastable) with respect to the bulk structures. Once a coherent superlattice is formed, it should remain stable. The tetragonal $(Mo)_1/(V)_1$ superlattices have the c axis parallel to the growth direction (see Fig. 1). We calculate total energies

TABLE III. Total energies for sc structures of $(Mo)_1/(V)_1$ with different lattice constants. The energy values are given as the difference between the superlattice total energy (per one Mo atom and one V atom) and the sum of the bulk total energies of Mo and V with calculated equilibrium lattice constants. The total pressure of sc $(Mo)_1/(V)_1$ with different lattice constants is also tabulated.

Lattice constant (Å)	$(Mo)_1/(V)_1$ Energy (eV)	Pressure (kbar)
3.10	−0.632	−13
3.09	−0.653	−9
3.07	−0.664	2
3.06	−0.662	7

for a configuration of six different choices for axis lengths (multiplied by the lattice constant), shown in Table IV. The energy values are given as the total-energy difference between the sc $(Mo)_1/(V)_1$ superlattice with lowest energy and the tetragonal $(Mo)_1/(V)_1$ superlattice. Negative values in Table IV indicate that the particular tetragonal structures are preferred to the optimal cubic one.

No absolute minimum is found within the area spanned by the points in Table IV and further efforts prove fruitless. The reason is that the system becomes unstable for too asymmetric structures, due to the ASA. Calculations of tetragonal elastic constants for bulk V and bulk Mo give reasonable results,[37] but they may not be transferable to the superlattice structures, where the elastic constants undergo changes, which means that the total-energy values for tetragonal Mo/V must be interpreted with care. Comparing total energies for tetragonal structures with unit cells that do not depart much from cubic unit cells, we notice that the tetragonal $(Mo)_1/(V)_1$ superlattice structures where there is a compression in the growth direction seem to be preferred to the sc structure. This has also been suggested in experimental and theoretical work[28,38] concerning the superconducting critical temperature of $(Mo)_n/(V)_n$ superlattices.

The severe limitations of the ASA when considering nonuniform distortions made us avoid total-energy computations of hydrogen in Mo/V superlattices. Calculations beyond ASA for hydrogen in such materials will be considered in a future work where one aim is also to compare rigorous calculations to the more approximate EMT scheme.

When we compare the properties of different $(Mo)_1/(V)_1$ superlattices, such as charge transfer, Fermi energy, and interstitial electron density, we see that the only property affected noticeably by the difference in the structures considered is the amount of charge transfer. One might then expect changes in the interstitial-density variation because of that but the effects of a volume-change on the density compensate the density effects of the charge-transfer change. Volume expansion acts to decrease the interstitial-electron density but to increase the electron transfer across the interface, giving negligible net effect on the interstitial-density value. Even computations where different sphere sizes and different interlayer spacings (for larger superlattices) were used did not show any dramatic changes in the results and in no case affected the conclusions regarding hydrogen solubility (within EMT) in these materials.

TABLE IV. Total energies for $(Mo)_1/(V)_1$ with tetragonal structure and different choices for the axis lengths. The z axis is directed along the growth direction (it is also the c axis of the tetragonal unit cell). The x and y axes are always chosen to have unit lengths and all axes are here multiplied with various lattice constants. The energy values are given as differences between the total energy for the tetragonal $(Mo)_1/(V)_1$ superlattices and the equilibrium sc $(Mo)_1/(V)_1$ superlattice.

	$(Mo)_1/(V)_1$	
x,y (Å)	z (Å)	Energy (meV)
3.05	3.09	37
3.08	3.07	1
3.07	3.06	−5
3.09	3.06	−10
3.07	3.05	−12
3.08	3.05	−18

IV. SUMMARY AND CONCLUSIONS

The electronic structure of $(Mo)_n/(V)_n$ metallic superlattices has been calculated for $n=1$, 3, and 5. The specific aim has been to study the valence-electron-distribution effects on hydrogen solubility in these materials, and the general aim has been to understand the valence-electron-character and lattice-structure effects on the electron structure in metallic superlattices.

The interstitial-electron-density variation in the superlattices is explored and, following effective-medium theory for hydrogen heat of solution in transition metals where the surrounding density is the key parameter,[14,15] it is found that the hydrogen solution is possible in every tetrahedral site in the vanadium layers of $(Mo)_n/(V)_n$ for $n \geq 3$. In experiments,[11] the interface vanadium layers in Mo/V are found to be almost hydrogen-free in a region of two to three layer spacings. The explanation given for the reduction of hydrogen solubility at the Mo/V interfaces also follows EMT arguments and is based on enhanced electron density at the interfaces due to electron transfer from Mo to V. We find here that there is a compensating effect—volume expansion of V—that allows H to have a negative absorption energy also at the interface vanadium layers. The observed reduction of hydrogen solubility cannot be explained by EMT arguments alone but may be sought in interdiffusion and relaxation at the interfaces and effects of H-H and H-metal interactions for higher H concentrations. The hydrogen concentration is expected to be modulated within the vanadium layers due to differences in H absorption energy in bulklike vanadium layers and in interface vanadium layers.

The band structure of the $(Mo)_n/(V)_n$ system in the Γ-Z direction is compared to the band structure of the bulk metals. Grossly, it can be understood in familiar terms of introduction of extra Bragg planes in the Brillouin zone where band folding and energy splitting of the bands are observed. The electron transfer at the interfaces follows intuitive rules also. Electrons flow from Mo to V in order to align the Fermi levels of the two metals. The character of the transferred electrons across the interfaces is mainly free-electron-like (s and p). Charge oscillations are seen because of the formation of a dipole layer at the interfaces due to the abrupt change of the effective potential. The local density of states of the superlattices show energy shifts—upwards for Mo and downwards for V—when going from bulklike to interface layers. This energy redistribution acts to adjust the LDOS peaks from their bulklike energy positions at the bulklike layers towards similar energy positions for the LDOS of interface molybdenum and interface vanadium. The LDOS shape is rather different for s and p electrons in the superlattices compared to the bulk shapes; this is

especially valid for interface atoms. The *d*-electron LDOS shape is somewhat more rigid within the superlattices for Mo and V atoms. They are, though, sensitive to the volume change which Mo and V undergo when forming a superlattice. The Mo *d*-electron band broadens due to volume expansion and, correspondingly, the V *d*-electron band becomes more narrow due to volume expansion. The volume changes also have the effect of changing the character of the valence DOS to more localized electrons in the case of volume contraction and more delocalized electrons in the case of volume expansion. Many of the above features have also been observed in electron structure calculations for other metallic superlattices[16] and give an indication of what can be expected when two metals are put together to form a superlattice.

The atomic-sphere approximation in the present calculations have certain implications with regard to the results. It is seen that in the calculations of equilibrium volume, the lattice constant is overestimated compared to KKR calculations[23] where nonoverlapping spheres were employed. Since both methods use muffin-tin potentials and the linearization of the eigenvalue equations in LMTO is expected to give a minor error, we believe that the ASA is the major cause of the overestimation of the equilibrium volume when no corrections for the sphere overlap are made (combined correction terms) and when the basis is limited to the usual *spd* basis. More severe is the limited types of crystal structures that can be considered for total-energy comparisons and the inhibition of including hydrogen impurities due to the inability of the ASA to treat nonuniform distortions. In the total-energy calculations, we are limited to considering cubic structures and tetragonal structures that do not depart much from cubic cells.

Restricting the geometric structure of the superlattices to be within a region where the ASA gives reasonable results, we find that a tetragonal distortion of the $(Mo)_1/(V)_1$ superlattice so as to compress it in the growth direction is favored over the sc structure, which is consistent with the findings of Karkut *et al.*[28] and Triscone *et al.*[38] Within this set of Mo/V superlattices, there are no property changes affecting the results and conclusions regarding interstital-electron-density variation and band structure. In a planned future study beyond ASA, properties of more crystal structures and hydrogen impurities will be considered.

ACKNOWLEDGMENTS

It is our pleasure to acknowledge Mats Persson for numerous valuable discussions and a critical reading of the manuscript. We would also like to thank Björgvin Hjörvarsson for bringing the problem of hydrogen solubility in metallic superlattices to our attention, and for many stimulating discussions. Financial support from NSC for the use of CRAY X-MP and from STU and NFR is gratefully acknowledged.

[1]V. Matijasevic and M. R. Beasley, in *Metallic Superlattices,* edited by T. Shinjo and T. Takada (Elsevier, Amsterdam, 1987), p. 187; K. Terakura, *ibid.*, p. 213.
[2]W. M. C. Yang, T. Tsakalakos, and J. E. Hilliard, J. Appl. Phys. **48**, 876 (1977).
[3]M. L. Huberman and M. Grimsditch, Phys. Rev. Lett. **62**, 1403 (1989).
[4]D. Wolf and J. F. Lutsko, Phys. Rev. Lett. **60**, 1170 (1988).
[5]B. M. Clemens and G. L. Easley, Phys. Rev. Lett. **61**, 2356 (1988).
[6]M. Grimsditch, Superlattices Microstruct. **4**, 677 (1988).
[7]J. R. Dutcher, S. Lee, J. Kim, G. I. Stegeman, and C. M. Falco, Phys. Rev. Lett. **65**, 1231 (1990).
[8]J. Mei and G. W. Fernando, Phys. Rev. Lett. **66**, 1882 (1991).
[9]S. Moehlecke, C. F. Majkrzak, and M. Strongin, Phys. Rev. B **31**, 6804 (1985).
[10]P. F.Miceli and H. Zabel, Z. Phys. B **74**, 457 (1989).
[11]B. Hjörvarsson, J. Rydén, E. Karlsson, J. Birch, and J.-E. Sundgren, Phys. Rev. B **43**, 6440 (1991).
[12]J. Birch, M. Severin, U. Wahlström, Y. Yamamoto, G. Radnoczi, R. Riklund, J.-E. Sundgren, and L. R. Wallenberg, Phys. Rev. B **41**, 10 398 (1990).
[13]M. G. Karkut, J.-M. Triscone, D. Ariosa, and Ø. Fischer, Phys. Rev. B **34**, 4390 (1986).
[14]J. K. Nørskov, Phys. Rev. B **26**, 2875 (1982).
[15]P. Nordlander, J. K. Nørskov, and F. Besenbacher, J. Phys. F **16**, 1161 (1986).
[16]H. v. Leuken, A. Lodder, M. T. Czyzyk, R. Springelkamp, and R. A. de Groot, Phys. Rev. B **41**, 5613 (1990).
[17]O. K. Andersen, Phys. Rev. B **12**, 3060 (1975).
[18]L. Hedin and B. I. Lundqvist, J. Phys. C **4**, 2064 (1971).
[19]J. Rath and A. J. Freeman, Phys. Rev. B **11**, 2109 (1975).
[20]W. R. L. Lambrecht, B. Segall, and O. K. Andersen, Phys. Rev. B **41**, 2813 (1990).
[21]T. Jarlborg and G. Arbman, J. Phys. F **7**, 1635 (1977).
[22]All experimental values for equilibrium lattice constants are taken from the Periodic Table in N. W. Ashcroft and N. D. Mermin, *Solid State Physics* (Holt, Rinehart and Winston International Editions, Philadelphia, 1976).
[23]V. L. Moruzzi, J. F. Janak, and A. R. Williams, *Calculated Electronic Properties of Metals* (Pergamon, New York, 1978).
[24]H. L. Skriver, *The LMTO Method* (Springer-Verlag, Berlin, 1984).
[25]B. Barbiellini, E. G. Moroni and T. Jarlborg, J. Phys. Condens. Matter **2**, 7597 (1990).
[26]N. Takeuchi, C. T. Chan, and K. M. Ho, Phys. Rev. B **40**, 1565 (1989).
[27]G. W. Fernando, R. E. Watson, M. Weinert, Y. J. Wang, and J. W. Davenport, Phys. Rev. B **41**, 11 813 (1990).
[28]M. G. Karkut, D. Ariosa, J.-M. Triscone, and Ø. Fischer, Phys. Rev. B **32**, 4800 (1985).
[29]B. W. Dodson, Phys. Rev. B **30**, 3545 (1984).
[30]F. Bechstedt and R. Enderlein, *Semiconductor Surfaces and Interfaces* (Akademie-Verlag, Berlin, 1988).
[31]T. Miller, M. Mueller, and T.-C. Chiang, Phys. Rev. B **40**, 1301 (1989).
[32]K. Papathanassopoulos and H. Wenzl, J. Phys. F **12**, 1369 (1982).

[33]H. Katsuta and R. B. McLellan, J. Phys. Chem. Solids **40**, 845 (1979).
[34]A. Zwartkruis and J. E. Himbergen, Surf. Sci. **214**, 1 (1989).
[35]M. Methfessel, C. O. Rodriguez, and O. K. Andersen, Phys. Rev. B **40**, 2009 (1989).
[36]H. L. Skriver, Phys. Rev. B **31**, 1909 (1985).
[37]O. Pictet, Ph.D. thesis, University of Geneva, 1989.
[38]J.-M. Triscone, D. Ariosa, M. G. Karkut, and Ø. Fischer, Phys. Rev. B **35**, 3238 (1987).

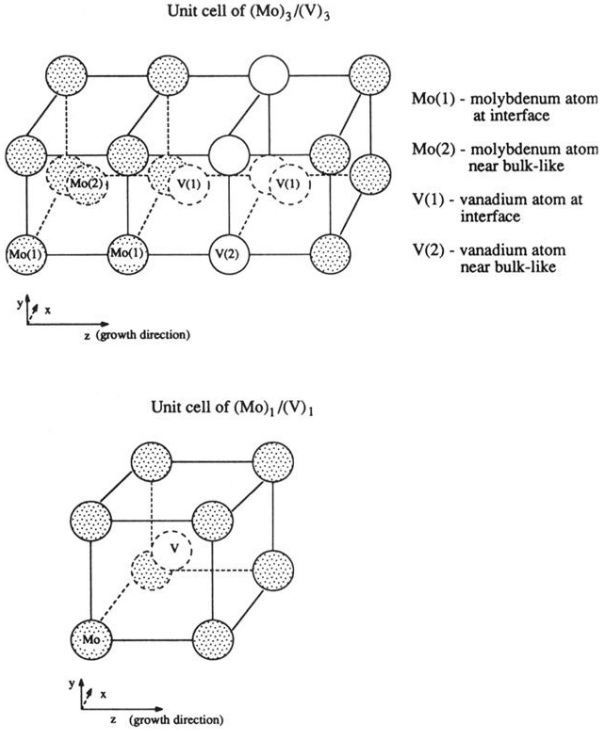

FIG. 1. Unit cells of $(Mo)_3/(V)_3$ and $(Mo)_1/(V)_1$ superlattices. The shaded atoms are Mo atoms, and the unfilled atoms are V atoms. The atoms labeled Mo and V [or Mo(1), Mo(2), V(1), and V(2)] are the ones constituting the unit cells.